

## ESR studies of the formyl radical in a CO matrix: Magnetophotoselective photolysis and thermally activated rotations

Frank J. Adrian, J. Bohandy, and B. F. Kim

Citation: *The Journal of Chemical Physics* **81**, 3805 (1984); doi: 10.1063/1.448182

View online: <http://dx.doi.org/10.1063/1.448182>

View Table of Contents: <http://scitation.aip.org/content/aip/journal/jcp/81/9?ver=pdfcov>

Published by the [AIP Publishing](#)

---

### Articles you may be interested in

[ESR studies of radical pairs of galvinoxyl radical in corresponding phenol matrix](#)

*J. Chem. Phys.* **72**, 598 (1980); 10.1063/1.438949

[ESR study of the photolysis of nbutyl iodide: Secondary photolysis and structure of the nbutyl radical](#)

*J. Chem. Phys.* **63**, 919 (1975); 10.1063/1.431411

[ESR Study of the Photolysis Products of HN<sub>3</sub> in an Inert Matrix: A Possible Rotating Triplet](#)

*J. Chem. Phys.* **42**, 2628 (1965); 10.1063/1.1696357

[Photolysis of the Phenoxy Radical in a Nitrogen Matrix](#)

*J. Chem. Phys.* **37**, 1974 (1962); 10.1063/1.1733414

[ESR Spectrum and Structure of the Formyl Radical](#)

*J. Chem. Phys.* **36**, 1661 (1962); 10.1063/1.1732794

---



# ESR studies of the formyl radical in a CO matrix: Magnetophotoselective photolysis and thermally activated rotations<sup>a)</sup>

F. J. Adrian, J. Bohandy, and B. F. Kim

*Milton S. Eisenhower Research Center, Applied Physics Laboratory, The Johns Hopkins University, Laurel, Maryland 20707*

(Received 26 March 1984; accepted 19 June 1984)

Photolysis of the formyl radical (HCO) in a CO matrix at 13 K by yellow light ( $\lambda > 500$  nm) polarized with its electric vector parallel to an external magnetic field ( $H_{DC}$ ) is orientationally selective, as shown by changes in the powder ESR spectrum of the radical. The depleted orientation in the cyclic photolysis [ $HCO \xrightarrow{h\nu} H + CO$ ;  $H +$  (a different CO)  $\rightarrow$  (randomly oriented HCO)] is (HCO plane)  $\perp H_{DC}$ , showing that the largest component of the optical transition moment is perpendicular to the HCO plane, as predicted by theory for a nonrotating HCO. Around 25 K part of the photoinduced orientational anisotropy is lost due to incipient rotation about an axis close to the CO bond, but the remaining orientational anisotropy persists to higher temperatures ( $\sim 40$  K), where it decays only slowly. Around 35 K this rotation becomes fast enough to yield a pseudoaxially symmetric powder ESR spectrum with  $g_{\parallel} = 1.9973$ ,  $g_{\perp} = 2.0021$ , and  $A_{\parallel} = A_{\perp} = 383.0$  MHz. The rotation axis is closest to but significantly different from the minimum inertial axis.

## I. INTRODUCTION

The randomly oriented free radical products of photochemical or radiolytic processes in inert gas matrices, glasses, and polymers typically present broad complex electron spin resonance (ESR) spectra known as powder patterns.<sup>1</sup> The sharp lines within these powder patterns correspond to radicals oriented so that the external magnetic field is approximately parallel to a magnetic axis, i.e., a principal axis of the tensor specifying the combined effects of the  $g$  factor and hyperfine anisotropies for a particular hyperfine splitting (hfs) line. The components of the  $g$  and hyperfine tensors can be determined from the positions of these peaks.

If such a randomly oriented radical has an optical transition with an anisotropic transition dipole moment, and if this transition leads to photolytic reaction or reorientation of the radical, then excitation of this transition with polarized light should produce a nonuniform orientational distribution of the radicals and, consequently, changes in the relative intensities of the principal-axis lines in the ESR powder pattern. This effect, which is known as magnetophotoselection, and heretofore has been observed in the photogeneration of metastable triplets in glassy media,<sup>2</sup> can provide information on the optical transition moment, the photochemical reaction mechanism, possible slow reorientation of the radical as a function of temperature, etc.

An obvious obstacle to these potentially interesting experiments is the requirement that the host medium be of sufficiently high optical quality that the exciting light is not completely depolarized by scattering. Glasses, together with some polymers, are the most promising media from the standpoint of optical quality, and recently we have observed orientational selectivity in the polarized-light photolysis of the formyl radical (HCO) in Suprasil 1 synthetic fused silica.<sup>3</sup>

Inert gas and other small-molecule matrices are more problematical because of their tendency to form microcrystalline snow-like deposits which scatter light strongly, but the versatility of these matrices for photochemical generation and trapping of reactive species makes their application in such experiments a potentially rewarding challenge. In this paper we show that polarized light photolysis of HCO in a CO matrix yields a small but informative anisotropy in the orientational distribution of the radicals. Also discussed is the reorientation of the radical about one axis at 30 to 35 K, which was observed during experiments on thermally activated decay of this orientational anisotropy.

## II. EXPERIMENTAL

The HCO radical was produced by ultraviolet (UV) photolysis (200 W high pressure Hg arc lamp) of a CO matrix containing 1% HI.<sup>4</sup> Using the apparatus described below, this matrix was formed by rapid condensation of the gaseous mixture into a 4 mm fused silica ESR tube cooled to 10 K in an Air Products Helitran helium flow-through cryostat equipped with a temperature controller. The cryostat was located in the ESR cavity of a home-built X-band ESR spectrometer. The samples were optically irradiated *in situ* through the slotted port in the Varian rectangular ESR cavity.

The matrix deposition apparatus consists of the following three elements. (1) A 250 ml gas sample preparation bulb with stopcocks leading to taper joint inlets and outlets, thereby enabling it to be attached to the vacuum line for filling and then removed for placement in the cryostat. (2) The sample tube consists of a 9 cm long, 4 mm o.d. diameter, Suprasil ESR tube fused to a 10 cm long, 7 mm o.d. diameter, silica tube which, in turn, is attached via a silica-to-Pyrex graded seal to a male 10/30 taper joint. (3) A short transition tube, which connects the sample tube to the bulb outlet, supports a narrow (1 mm i.d. diameter) inlet tube which inserts into the

<sup>a)</sup> Work supported by the U. S. Naval Sea Systems Command under Contract No. N00024-83-C-5301.

sample tube and comes to within 2.5 cm of its bottom when the sample tube is attached to the transition tube. This inlet tube is supported by a Teflon collar which rests on the neck of the female 10/30 taper joint which accepts the sample tube taper joint, and it is centered in the sample tube by small Teflon rings. During deposition of a matrix the gas pressure in the sample bulb pushes the inlet tube support collar against the neck of this taper joint creating a seal which forces the bulk of the depositing gas down the inlet tube to the bottom of the sample tube. In the event of an inadvertent pressure build up in the sample tube, however, this collar would be pushed up allowing the expanding gas to escape back to the sample bulb. This apparatus is supported in the cryostat by a saddle which rests on the magnet pole faces. A split Teflon collar, girded by three "O" rings which hold it firmly on the female taper joint at the bottom of the transition tube (where the sample tube is attached), fits snugly into a cylindrical ring on the saddle, thereby supporting the apparatus, centering the sample tube in the Helitran tube, and allowing the sample tube to be rotated within the ESR cavity.

With this apparatus, a matrix is formed by filling the sample bulb with the desired gas mixture, transferring the apparatus to the cryostat and, after waiting several minutes for the sample tube to reach the ambient cryogenic temperature, opening the outlet stopcock allowing the gas mixture to expand through the inlet tube and condense in the bottom of the sample tube. Inspection of the deposited CO:HI matrix, made immediately after sudden withdrawal of the sample tube from the cryostat, revealed a semitranslucent matrix. Although this matrix obviously scattered light to a considerable degree, it appeared to be optically superior to the snowy microcrystalline matrices which usually result from slow condensation of a gas at low pressures onto a cold finger. No effort was made in these first experiments to investigate matrix optical quality as a function of deposition rate, temperature, etc., although this appears to be a worthwhile line of investigation given the results we now discuss for this rather crude matrix deposition process.

### III. RESULTS AND DISCUSSION

#### A. Magnetophotoselective photolysis of HCO

The HI:CO matrix was UV photolyzed at 13 K until the HCO ESR signal stopped growing ( $\sim 15$  min) and was then annealed briefly at 25 K and returned to 13 K. At this point the high and low field members of the HCO hfs doublet were as shown in Figs. 1(a) and 2(a), respectively. This spectrum is very similar to that observed in the original experiment where the matrix was prepared by low-pressure vapor deposition onto a sapphire rod.<sup>4</sup> Analysis of the original spectrum showed that the  $x$  principal axis is perpendicular to the molecular plane and the  $z$  axis is approximately along the CO bond.<sup>4</sup> No hydrogen atom ESR spectra were observed either at this point or following visible-light photolysis of the HCO radicals, which indicates that all H atoms react with CO matrix molecules irregardless of whether they are formed by photolysis of HI or HCO.

A  $90^\circ$  rotation of the sample tube about its axis did not change the spectrum in Fig. 1(a), which test indicated that this initial ensemble of radicals was randomly oriented, as might be expected from the UV-induced photochemical reaction ( $\text{HI} \xrightarrow{h\nu} \text{H} + \text{I}$ ;  $\text{H} + \text{CO} \rightarrow \text{HCO}$ ). Furthermore, this test, and other tests involving successive observations of the ESR spectrum of the same sample, showed that the changes produced by photolysis of HCO with visible polarized light, which we discuss next, cannot be artifacts of instrumental noise, temperature instability, or other factors which can lead to variations in successive runs of the same ESR spectrum.

On the other hand, it should be noted that even unpolarized light can produce an orientational anisotropy if a magnetophotoselective process such as secondary photolysis of the HCO radicals occurs. This is because in our optical geometry unpolarized light has components parallel and perpendicular to the tube axis, which latter component may produce an orientational anisotropy with respect to rotation of the sample tube. There are weak indications of such orientational anisotropy in samples which were subjected to longer photolysis, with consequent greater secondary photolysis of the primary HCO radicals, and/or were not annealed, which process, as we discuss later, partially removes the photoinduced anisotropy.

Figure 1(b) shows the high field HCO line after photolysis.

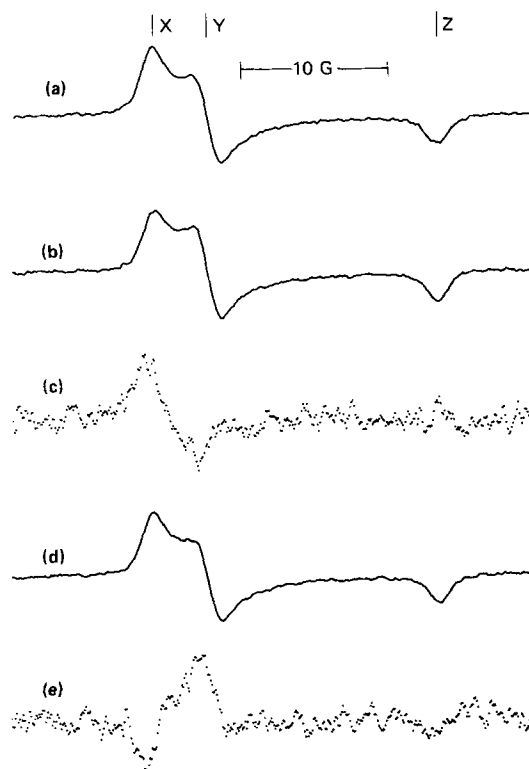


FIG. 1. Effect of polarized visible light photolysis with  $\mathbf{E}_0 \parallel \mathbf{H}_{\text{DC}}$  on the high-field ESR line of HCO in CO at 13 K. (a) Unphotolyzed line. (b) After photolysis. (c) Difference spectrum: (a) minus (b). Ordinate scale is six times that used for a and b. (d) Effect of rotating the photolyzed sample  $90^\circ$  about the axis perpendicular to both  $\mathbf{H}_{\text{DC}}$  and the direction of the photolyzing light. (e) Difference spectrum: (b) minus (d). Ordinate scale is six times that used for a, b, and d.

sis of this sample for 6 min with visible light in the wavelength region  $\lambda > 500$  nm (Hg arc lamp with a Corning C.S. 3-70 filter), and polarized with the optical electric vector ( $E_O$ ) parallel to the external magnetic field ( $H_{DC}$ ). This spectrum was unchanged by further photolysis, indicating that an equilibrium condition had been reached. Visual comparison of Figs. 1(a) and 1(b), and comparison of the difference spectrum [(spectrum 1a) minus (spectrum 1b)], given in Fig. 1(c) with line shape calculations in Fig. 3, show that the photolysis decreased the intensity of the  $x$  principal-axis line while increasing the intensity of the  $y$  line. The difference spectrum also contains a weak line in the  $z$  position indicative of a photolytic increase in the  $z$  component of the high field HCO line, but the signal to noise is too low for a definite conclusion in this case.

The photolytic increase in the  $z$  principal-axis line was confirmed using the low field member of the HCO hfs doublet, which has the advantage of being a more compact and thus more intense powder pattern than its high field counterpart, although less informative than the latter because of the accidental coincidence of the  $x$  and  $y$  principal-axis lines to yield an axially symmetric-like pattern. Upon polarized light photolysis the low field powder pattern changed from the solid curve to the dotted curve in Fig. 2(a), where the assignments of the  $x$ ,  $y$ , and  $z$  principal axis lines relative to those of the high field powder pattern have been established previously.<sup>4</sup> Clearly there has been an increase in the  $z$  component at the expense of the combined  $x$  and  $y$  components. This change is also apparent in the difference spectrum [(unphotolyzed line) - (photolyzed line)] shown in Fig. 2(b). Finally, as we discuss in more detail later, the total intensity of the HCO ESR spectrum is unchanged by the visible light photolysis so the line shape changes are completely due to

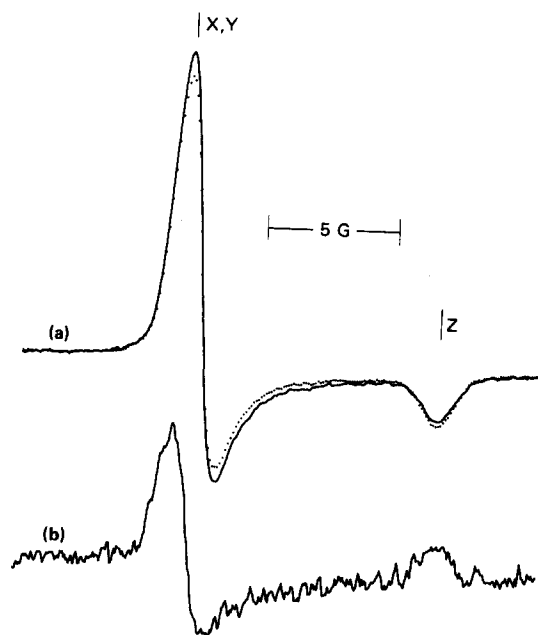


FIG. 2. Effect of polarized visible light photolysis with  $E_O \parallel H_{DC}$  on the low field ESR line of HCO in CO at 13 K. (a)—Unphotolyzed line; ---after photolysis. (b) Difference spectrum: (unphotolyzed spectrum) minus (photolyzed spectrum). Ordinate scale is five times that used for a.

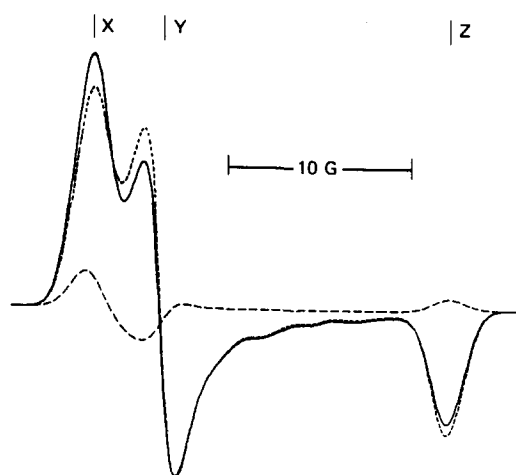


FIG. 3. Calculated ESR powder pattern for the high field member of the HCO hfs doublet. —Randomly oriented radical; ---partially oriented radical with the  $x$  intensity 20% less than its random value and the  $y$  and  $z$  intensities 10% greater than their random values; --- (random spectrum) minus (partially oriented spectrum).

magnetophotoselective transfer of intensity between radical orientations.

Figures 3 and 4 show, for the high and low field members of the HCO hfs doublet, respectively, calculated ESR powder patterns for a randomly oriented ensemble of radicals (solid curves) and for a photoinduced orientational anisotropy corresponding to a 20% reduction in radical concentration at the orientations corresponding to the  $x$  principal-axis line and a 10% increase in concentration at the orientations yielding the  $y$  and  $z$  lines. (short-dashed curves). The calculated difference spectra [(random spectrum) - (photo-oriented spectrum)] are also shown in these figures (long dashed curves). The calculations used a modification of the method of Lefebvre,<sup>5</sup> as previously discussed,<sup>3</sup> with the orientation distribution functions

$$f_r(\theta, \phi) = (\sin \theta / 4\pi)$$

and

$$f_p(\theta, \phi) = (\sin \theta / 4\pi) \exp[0.095(\cos^2 \theta + \sin^2 \theta \sin^2 \phi) - 0.22 \sin^2 \theta \cos^2 \phi]$$

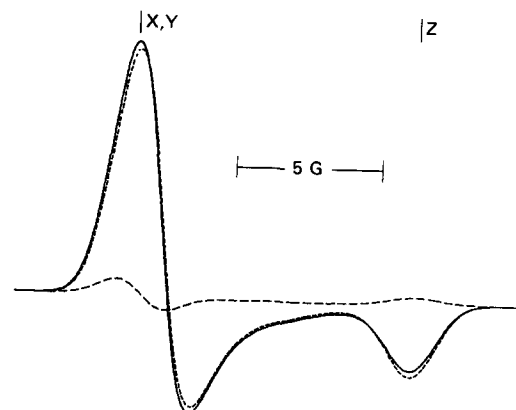


FIG. 4. Calculated ESR powder pattern for the low field member of the HCO hfs doublet.—randomly oriented radical; ---partially oriented radical with  $x$  intensity 20% less than its random value and the  $y$  and  $z$  intensities 10% greater than their random values; --- (random spectrum) minus (partially oriented spectrum).

for the random and partially photo-oriented cases, respectively. Here,  $\theta$  and  $\phi$  are the polar and azimuthal angles specifying the orientation of the external magnetic field with respect to the principal axes of the radical. The HCO magnetic constants used in the calculation have been determined previously<sup>4</sup> and are given in Table I. The symmetric part of the line broadening was taken to be a Gaussian with a root-mean-square width of 0.9 G. The agreement between the observed and calculated spectra is quite good, where, in comparing, it is to be noted that the experimental difference spectra are plotted on expanded ordinate scales which are six and five times the ordinate scales used for the actual spectra in Figs. 1 and 2, respectively. This comparison of observed and calculated spectra also indicates that the photolysis produces roughly a 20% nonuniformity in the orientational distribution of the radicals. A magnetophotoselective effect of this magnitude is consistent with the aforementioned visually determined mediocre optical quality of the matrix and consequent depolarization of the light by scattering.

As shown in Fig. 1(d) for the high field line, rotation of the polarized-photolysis sample 90° about the tube axis, which direction is perpendicular to both  $H_{DC}$  and the direction of the light, confirms the presence of a photoinduced nonuniform distribution of orientations. Here, as is visually apparent in the region of the  $x$  and  $y$  principal-axis lines and in the difference spectrum, [(spectrum 1b) minus (spectrum 1d)], given in Fig. 1(e), the rotation tends to reverse the magnetophotoselective effect of the photolysis, that is, the intensity of the originally depleted  $x$  component is increased at the expense of the less photodepleted  $y$  component. Tube rotation had a similar effect (not shown in Fig. 2) on the low field line, with the photodepleted  $x, y$  component increasing at the expense of the less photodepleted  $z$  component. A weak indication of this  $z$ -component change is present in Fig. 1(e), but the signal to noise is too poor for a definite conclusion in this case. This test eliminates the possibility that the photoinduced line shape changes are due to such photolysis artifacts as changes in linewidth, matrix site, etc., since these cannot produce orientation dependence in the ESR spectrum of the photolyzed sample. Sample rotation will also be very useful for investigating magnetophotoselective effects in cases where the photolysis reduces the total spectral intensity, which complicates comparison of the pre- and post-photolysis spectra, whereas the total intensity of the post-photolysis spectrum should be orientation independent [this was confirmed by double integration of the spectra in Figs. 1(b) and 1(d)]. Furthermore, as we discuss momentarily, use of the

orientation dependence of the spectrum to determine orientational anisotropy enables observation of very low frequency radical reorientations via the consequent decay of this anisotropy.

The total intensities of the original and photolyzed spectra in Figs. 1(a) and 1(b), determined by double integration of the ESR absorption derivatives, are equal within the estimated 5% error limits of this procedure. The original and photolyzed spectra in Fig. 2 are also equal within these error limits. This strongly suggests that all the H atoms produced by the HCO photolysis recombine with other CO molecules but that the HCO molecules so formed are randomly oriented. An alternate possibility is that the photoexcited HCO molecule rotates in the excited state and returns to the ground state in a new random orientation. This second possibility is less likely because the same photolysis of HCO in fused silica, where the photolytic H atoms cannot all react with CO, caused a decrease in the total ESR intensity.<sup>3</sup> It would be interesting, however, to test the effect of photolysis at photon energies less than the 1.7 eV dissociation energy of the CH bond in this radical. Both these mechanisms yield the same result under polarized light photolysis, namely, a transfer of intensity from the most to the least readily photolyzed orientations, without changing the total intensity. This is the ideal situation for experiments in matrices where the light is largely depolarized by scattering, because the correspondingly small changes in the intensities of the principal-axis components of the ESR powder pattern will be easier to observe if the overall intensity of the line is not reduced by irreversible photodecomposition.

For the  $E_0 \parallel H_{DC}$  geometry the relative photolytic intensity reduction of the  $i$ th principal-axis component of a powder ESR spectrum will be proportional to  $\mu_{0i}^2$ , where  $\mu_{0i}$  is the component of the optical transition moment  $\mu_0$  along the  $i$ th axis.<sup>3</sup> The observed results, i.e., reduction of the  $x$  component relative to the  $y$  and  $z$  components, are consistent with the facts that the  $x$  axis is perpendicular to the HCO plane<sup>4</sup> and that  $\mu_{0x}$  is the largest component of  $\mu_0$  for the  ${}^2A' \leftarrow {}^2A'$  transition in a nonrotating HCO molecule.<sup>6,7</sup>

## B. Thermally activated rotations and pseudoaxially symmetric HCO

As mentioned previously, comparison of the ESR spectra at the 0° and 90° orientations of the sample tube enables measurement of the photoinduced orientational anisotropy as a function of temperature. Observations on the high field line showed that the  $x$ - $y$  anisotropy weakened on going from 13 to 20 K and disappeared around 25 K. On the other hand, observations on the low field line showed that the  $(x, y)$ - $z$  anisotropy persisted to considerably higher temperatures. Rough measurements, made by observing the anisotropy at 13 K, warming to a higher temperature for a few minutes and recooling and remeasuring at 13 K, indicated that this anisotropy persists to about 40 K, at which point the radical itself is slowly decaying.

Although the foregoing measurements are only qualitative they are in accord with the expectation that the radical will first reorient about an axis close to the CO bond (since this involves primarily motion of the light H atom and can

TABLE I. Magnetic constants of the low-temperature nonaxially symmetric and high-temperature pseudoaxially symmetric forms of HCO in a CO matrix.  $A$  for the nonaxial case is in the principal axis system of  $g$ . All hfs values are in MHz and second-order hfs corrections were included in calculating the  $g$  factors.

Fixed HCO radical	Rotating HCO radical
$A_{xx} = 372.1, \quad g_x = 2.0041$	$A_{\perp} = 383.0, \quad g_{\perp} = 2.0021$
$A_{yy} = 381.7, \quad g_y = 2.0027$	$A_{\parallel} = 383.0, \quad g_{\parallel} = 1.9973$
$A_{zz} = 397.9, \quad g_z = 1.9960$	
$ A_{yz}  = 16.2$	

occur by tunneling as well as classically), which motion will remove any orientational anisotropy with respect to the  $x$  and  $y$  axes which are approximately perpendicular to the CO bond. Removal of the orientational anisotropy with respect to  $(x, y)$ - $z$  axes, on the other hand, requires reorientation about an axis which is approximately perpendicular to the CO bond.

At roughly 35 K this reorientation becomes fast enough to average out the magnetic differences between the  $x$  and  $y$  principal axes and the spectrum changes from a nonaxially symmetric to a pseudoaxially symmetric powder ESR spectrum. The limiting low and high temperature spectra are shown in Figs. 5(a) and 5(b), respectively. At intermediate temperatures between 28 and 35 K both forms are present. Continued warming beyond 35 K caused the radical to decay; in fact, the HCO ESR intensity is very slowly decreasing at 35 K. The field positions of the principal axis lines in the low-temperature nonrotating HCO radical are, within experimental error of approximately 0.2 G, the same as those observed previously, where the components of the hyperfine splitting (hfs) tensor ( $\mathbf{A}$ ) and the  $g$  factor tensor ( $\mathbf{g}$ ) were determined from a more complete analysis of the ESR spectra of both HCO and DCO.<sup>4</sup> These results, together with the values of  $\mathbf{A}$  and  $\mathbf{g}$  for the high temperature rotating radical, are given in Table I. It is noteworthy that this rotation completely removes the hyperfine anisotropy, leaving only a  $g$ -factor anisotropy.

If components and principal axes of the  $g$  tensor and the anisotropic part of the proton hfs tensor ( $\mathbf{B}$ ) are known for the nonrotating radical, then the rotation axis can be determined from the corresponding values of these tensors in the rotating radical. The relevant equations, derived by transforming  $\mathbf{g}$  and  $\mathbf{B}$  from an axis system in the rigid radical to a system in which the new  $z$  axis is the rotation axis, are:

$$g_{\parallel} = g_x \sin^2 \theta_r \cos^2 \phi_r + g_y \sin^2 \theta_r \times \sin^2 \phi_r + g_z \cos^2 \theta_r, \quad (1a)$$

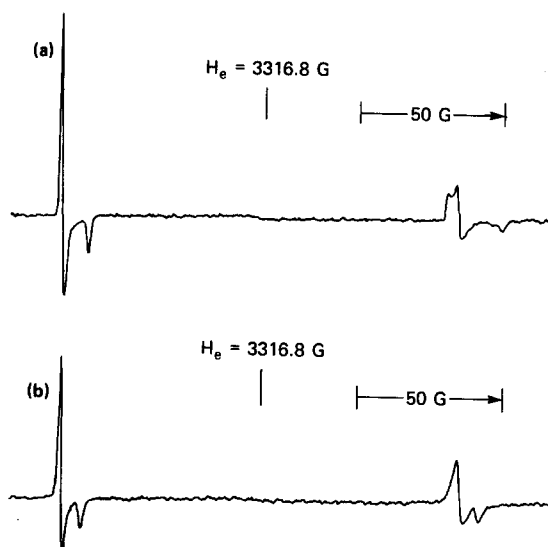


FIG. 5. (a) ESR spectrum of HCO in CO at 19 K. (b) ESR spectrum of HCO in CO at 35 K.  $H_e$  is the resonant field strength of the free electron.

$$B_{\parallel} = (B_{xx} \cos^2 \phi_r + B_{yy} \sin^2 \phi_r) \sin^2 \theta_r + B_{yz} \sin \phi_r \sin 2\theta_r + B_{zz} \cos^2 \theta_r, \quad (1b)$$

where, as shown in Fig. 6, the components of  $\mathbf{B}$  are in the principal axis system of  $\mathbf{g}$ , and  $\theta_r$  and  $\phi_r$  are the polar and azimuthal angles of the rotation axis ( $\Omega_r$ ) in this axis system.

The only symmetry-determined principal axis in HCO is the  $x$  axis, which is perpendicular to the molecular plane. The theory of  $g$  shifts in HCO locates the  $g_z$  axis approximately along the CO bond,<sup>4</sup> however a more precise location of the principal axes of  $\mathbf{g}$  is desirable for determining the rotation axis from Eq. (1) and the values of  $\mathbf{g}$  and  $\mathbf{B}$  in the fixed and rotating radical. To locate the principal axes of  $\mathbf{g}$ , and also to determine the needed sign of the off-diagonal hfs component  $B_{yz}$  in this axis system, we utilize a recent *ab initio* calculation of the HCO hfs constants<sup>8</sup> together with a microwave spectroscopic determination of the components of  $\mathbf{B}$  along the principal inertial axes of the free molecule,<sup>9</sup> which axes are known precisely.<sup>10</sup> Transformation of the calculated  $\mathbf{B}$  ( $B_{x'x'} = -17.4$ ,  $B_{y'y'} = 24.9$ , and  $B_{z'z'} = -7.6$  MHz, where  $x'$  is perpendicular to the molecular plane and  $y'$  is approximately along the CH bond)<sup>8</sup> into the principal axis system of  $\mathbf{g}$  shows that  $B_{yz}$  is negative for any reasonable choice of the principal axes of  $\mathbf{g}$ , if the positive directions of these axes are as shown in Fig. 6. Then, the best agreement between the experimental values of  $\mathbf{B}$  for HCO in a CO matrix ( $B_{xx} = -11.8$ ,  $B_{yy} = -2.2$ ,  $B_{yz} = -16.2$ , and  $B_{zz} = 14.0$  MHz where  $a$ ,  $b$ , and  $c$  are the principal inertial axes)<sup>9</sup> is obtained when, as shown in Fig. 6, the  $g_z$  axis makes an angle of  $7^\circ$  with the minimum inertial axis ( $a$ -axis) and, consequently, an angle of  $13.4^\circ$  with the CO bond. For this choice of the principal axes of  $\mathbf{g}$  the observed  $\mathbf{B}$  for HCO in CO yields  $B_{aa} = 9.8$ ,  $B_{bb} = 2.0$ , and  $B_{cc} = -11.8$  MHz, in reasonably good agreement with the microwave data.

Thus, using in Eq. (1) the experimental values of  $\mathbf{g}$  and  $\mathbf{B}$  in the rigid radical, with  $B_{yz}$  negative, we have calculated as functions of  $\phi_r$  the values of  $\theta_r$ , denoted  $\theta_r^{(g)}$  and  $\theta_r^{(B)}$ , which respectively satisfy the experimental results:  $g_{\parallel} = 1.9973$  and  $B_{\parallel} = 0$  in the rotating radical. The  $\theta_r^{(g)}$  and  $\theta_r^{(B)}$  vs  $\phi_r$  curves, given in Fig. 7, intersect at approximately  $\theta_g = 25^\circ$  and  $\phi_g = 58^\circ$ , which should determine the rotation axis, but, unfortunately, the location of this intersection is very imprecise and subject to large variations for small changes in the experimental data. This occurs because the  $\theta_r^{(g)}$  and  $\theta_r^{(B)}$  val-

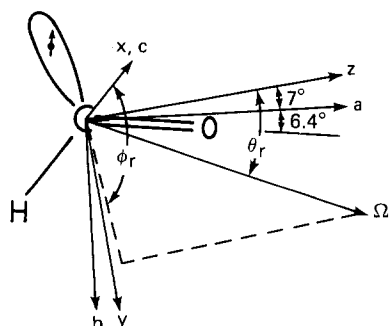


FIG. 6. Illustration of the  $g$ -factor principal axes ( $x, y, z$ ), the principal inertial axes ( $a, b, c$ ) and the rotation axis ( $\Omega_r$ ) of HCO in CO.

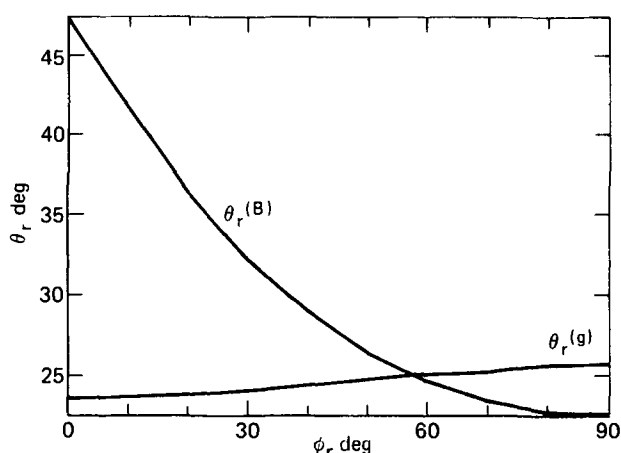


FIG. 7. Plots of  $\theta_r^{(g)}$  and  $\theta_r^{(B)}$  vs  $\phi_r$ .

ues are within  $3^\circ$  of each other, in the range  $23^\circ > \theta_r > 27^\circ$  for a wide range of  $\phi_r$  values, namely,  $45^\circ < \phi_r < 135^\circ$ . Consequently,  $\Omega_r$  can be located only within these wide limits of  $\phi_r$ , where it is to be noted that  $\phi_r = 90^\circ$  and  $\theta_r = 23^\circ$  places the rotation axis in the  $y$ - $z$  plane and between the CH and CO bonds.

This  $\phi_r = 90^\circ$  assignment of  $\Omega_r$  is the most reasonable since it is closest to the inertial axis  $a$ , which corresponds to the lowest moment of inertia of HCO and there is a general tendency for the initial rotation of a matrix-isolated radical to be about the minimum inertial axis. Even with the large uncertainty in the location of the rotation axis, however, it must differ considerably from the  $a$  axis, otherwise the proton hfs anisotropy in the pseudoaxially symmetric radical would be approximately 11.6 MHz, corresponding to  $B_{aa}$ ,<sup>9</sup> rather than the observed value of zero. Thus, matrix interactions appear to play a strong role in determining the rotation axis and may also be the reason why the rotation occurs only after warming to about 35 K, in contrast to the behavior of many matrix-isolated radicals which rotate about low moment-of-inertia axes even at 4 K.

The warmup behavior just described differs significantly from that of the original system of HCO in a CO matrix deposited on a cold finger,<sup>4</sup> even though the low-temperature spectra and magnetic constants are identical in the two

systems. In the original system the spectrum broadened on warmup and never exhibited the well-resolved pseudoaxial spectrum of Fig. 5(b). The reasons for this difference are not understood, but, given that the effects of a uniaxial rotation of HCO depend strongly on the direction of the rotation, it is possible that a slight variation among matrix trapping sites and a corresponding spread of rotation axes could lead to the observed broadening in the original system. These results do show that there can be significant differences between matrices prepared by condensing into a cold tube vs condensation onto a cold finger, and that the former method may have advantages in some cases.

In summary, the present results on magnetophotoselective photolysis of HCO in a CO matrix of rather mediocre optical quality indicate that this will be a useful method for investigating photochemical reactions involving matrix isolated species, particularly in the likely event that matrix optical quality can be improved by suitable choice of such deposition conditions as flow rate, temperature, shape of the ESR tube, etc.

#### ACKNOWLEDGMENT

The authors are indebted to Mr. P. R. Zarriello for his capable assistance with these experiments.

- <sup>1</sup>P. B. Ayscough, *Electron Spin Resonance in Chemistry* (Methuen, London, 1967), Chap. 9.
- <sup>2</sup>S. P. McGlynn, T. Azumi, and M. Kinoshita, *Molecular Spectroscopy of the Triplet State* (Prentice Hall, Englewood Cliffs, 1969), pp. 364–368.
- <sup>3</sup>J. Bohandy, B. F. Kim, and F. J. Adrian, *Chem. Phys. Lett.* **104**, 413 (1984).
- <sup>4</sup>F. J. Adrian, E. L. Cochran, and V. A. Bowers, *J. Chem. Phys.* **36**, 1661 (1962).
- <sup>5</sup>R. Lefebvre, *J. Chem. Phys.* **33**, 1826 (1960).
- <sup>6</sup>G. Herzberg and D. A. Ramsay, *Proc. R. Soc. London Ser. A* **233**, 34 (1955).
- <sup>7</sup>J. W. C. Johns, S. H. Priddle, and D. A. Ramsay, *Discuss. Faraday Soc.* **35**, 90 (1963).
- <sup>8</sup>D. Feller and E. R. Davidson, *J. Chem. Phys.* **80**, 1006 (1984).
- <sup>9</sup>B. J. Boland, J. M. Brown, and A. Carrington, *Mol. Phys.* **34**, 453 (1977).
- <sup>10</sup>J. M. Brown and D. A. Ramsay, *Can. J. Phys.* **53**, 2232 (1975).